

Opportunities for materials science: From molecules to neural networks

Giovanni Zocchi

This article addresses why biomaterials are a growing part of materials science. We consider two areas at two different scales. At the nanometer scale, enzymes are heterogeneous nanoparticles of extraordinary deformability; this property allows us to view biomolecules informed by concepts of materials science and nonlinear physics. A degree of universality in the mechanical behavior of the molecules appears in the ubiquitous softening transitions; some results obtained dynamically by nanorheology, and others obtained in equilibrium experiments through the method of the DNA springs are summarized. These soft molecules represent an opportunity for studies of dissipation at the atomic scale. At the mesoscopic scale, composite functional materials with biological components hold promise for applications such as low power, chemically driven, biodegradable devices. A concrete example, and a program for the future, is the artificial axon. It is a synthetic structure that supports action potentials based on the same physical mechanism as the voltage spikes in nerve cells. A network of such axons, which is yet to come, would constitute an artificial brain. Beyond device applications, the focus here is on the basic science, namely, a constructivist approach to cybernetics, algorithmic mathematics, and the brain.

Introduction

Biomaterials have long been an important part of materials science and engineering. Constructions and objects made of wood, bone, and cotton for thousands of years were augmented and replaced with metals, on an industrial scale, in the past 150 years, and with synthetic polymers and silicon fairly recently. Today, we may be standing at the threshold of a new era in materials science and technology, with engineered biomaterials augmenting and replacing plastic and electronic devices, and driving innovation. Previous revolutions in materials science came at the cost, we now know, of local and global ecological disasters—from the copper mines of Chile to plastic in the oceans. Engineered biomaterials have the potential of evolving into an eco-friendly sector of the economy outputting biodegradable products. Specifically, the combination of biomaterials and molecular-scale manufacturing—artificial life minus self-reproduction—could drive new engineering directions, especially in the general area of devices.¹ Examples include smart tissue implants, miniaturized mechanochemical actuators (such as artificial muscles), and in general active materials which react to changes in their physical or chemical environments.

As with nanoscience in general, the direction that eventual large-scale applications will take is difficult to foresee. What is clear even now is the capability of the field for generating

new science. In a general sense, the problems being addressed encompass more than one field of physics, with a focus on those fields we understand least. In keywords, these are far-from-equilibrium, nonlinear, complex systems. As an example, the working of an enzyme, which is one big catalyst molecule, results from mechanochemical coupling within the material, in an environment with out-of-equilibrium concentrations of reactants. Nonequilibrium is of the essence, similar in this respect to a driven turbulent flow, and different from situations such as currents in conductors, where the material is locally in equilibrium. Similarly, the active gel that forms the cytoskeleton (the polymer network that provides the structural support to the cell) is fundamentally maintained by nonequilibrium processes such as treadmilling (the process by which an actin filament, for example, displaces itself by polymerizing at one end while depolymerizing at the opposite end).² When we consider biomaterials from the point of view of the nonequilibrium processes that maintain them and the nonlinearities that underlie their functions, we see new opportunities for materials science at different scales, from the molecular to the macroscopic.

Big molecules as materials

A typical monomeric enzyme is a composite solid-like nanoparticle about 4 nm in size, consisting of $\sim 10^4$ atoms. Its bond

Giovanni Zocchi, Department of Physics, University of California, Los Angeles, USA; zocchi@physics.ucla.edu
doi:10.1557/mrs.2019.23

structure is different from a solid-state nanoparticle. Namely, the covalent bond structure is that of a polymer chain made of amino acids. This chain is folded into an ordered, solid-like particle by competing interactions, each of which are about 100 times weaker than a covalent bond—namely, hydrogen bonds, van der Waals interactions, and entropic forces such as hydrophobicity. There are two main consequences that distinguish these “soft” particles from the solid-state ones. One is that because of the nanometer size and weak internal bonds, surface energies are on the same order as bulk energies and, therefore, surface effects are important, if not dominant. For example, the enzyme nanoparticle structure described is stable in water, but not in a hydrophobic solvent or even at a water–air interface. As a result, the protein–water interface—that is, the hydration layer (the first layer of water molecules surrounding the protein)—must be considered as part of the molecule.^{3–7}

The other consequence is the extraordinary deformability of the nanoparticles. A ~ 40 Å size enzyme can typically be reversibly deformed by 3–4 Å, corresponding to strains on the order of 10%.⁷ For comparison, a typical yield strain for a solid is on the order of 0.1%, beyond which the material deforms irreversibly. We should think of large deformations of enzymes as similar to plastic deformations in solids, but reversible; or else as a fracture problem, again reversible. The microscopic mechanism underlying the deformation is the breaking and reforming, in a different pattern, of those weak bonds, say hydrogen bonds, which hold the nanoparticle together. Molecular biologists refer to these processes as conformational changes. They have been predicted⁸ and demonstrated experimentally by x-ray crystallography^{9,10} some 50 years ago, and studied intensively ever since.

What is new that might justify the attention of materials scientists toward these well-studied, well-established processes? Roughly speaking, and exceptions notwithstanding, up until recently, deformations of enzymes were merely observed statically by viewing the structure using x-ray crystallography before and after the deformation. Enzymes are molecular machines that go through a cycle of deformations as they catalyze a specific chemical reaction. Binding of the reactants to the enzyme, and unbinding of the products, drives the conformational changes. It is thus possible to prepare an enzyme in different conformational states through binding to different ligands, and observe these different conformations by x-ray crystallography, nuclear magnetic resonance structure determinations, or other means. However, it is only over the past 10 years that methods were introduced to drive enzyme deformations through “external fields,” mainly force fields provided by DNA springs, under the experimenter’s control.^{11–13} This development is releasing the investigator from the fetters of considering only the naturally occurring, ligand-driven conformational changes, where the “applied stresses” are difficult to quantify and impossible to control.

We now know that large amplitude, reversible enzyme deformability is by no means confined to the conformational

changes elicited by ligand binding.^{13–16} Different applied stresses elicit different deformations, as opposed to biasing the structure toward one or the other specific conformation, which results from ligand binding. In short, the enzyme behaves mechanically more like a blob of jelly than clockwork. Correspondingly, some traditional materials science techniques, suitably revised to deal with the nanometer scale, offer a new window on the physical properties of these complex molecules.

One such technique is nanorheology.^{12,16–18} This method has been used to perform rheology measurements on enzyme molecules: one applies an oscillatory stress to the molecules and measures the amplitude and phase of the resulting strain. **Figure 1**¹⁹ shows one interesting feature that emerges. The amplitude of the applied force versus the measured amplitude of the deformation is displayed for the ~ 4 -nm enzyme guanylate kinase, sandwiched between the two “plates” of the

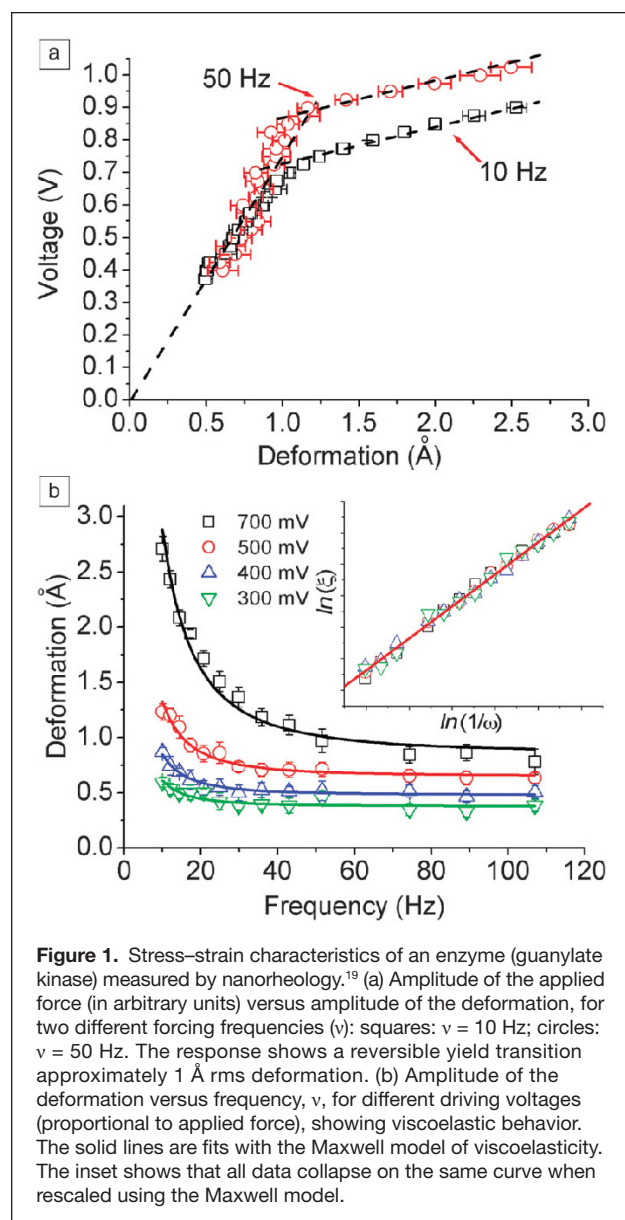


Figure 1. Stress–strain characteristics of an enzyme (guanylate kinase) measured by nanorheology.¹⁹ (a) Amplitude of the applied force (in arbitrary units) versus amplitude of the deformation, for two different forcing frequencies (ν): squares: $\nu = 10$ Hz; circles: $\nu = 50$ Hz. The response shows a reversible yield transition approximately 1 Å rms deformation. (b) Amplitude of the deformation versus frequency, ν , for different driving voltages (proportional to applied force), showing viscoelastic behavior. The solid lines are fits with the Maxwell model of viscoelasticity. The inset shows that all data collapse on the same curve when rescaled using the Maxwell model.

“rheometer.” The linear elasticity regime (which extrapolates to the origin) is cut off by a reversible yield transition at ~ 1 Å rms deformation. The transition is frequency dependent. Another interesting feature is seen in the frequency behavior of the deformation amplitude (Figure 1b). The amplitude increases as $\sim 1/\omega$ at low frequency, ω , and shows generally the features of viscoelastic dynamics (the solid lines represent the Maxwell model of viscoelasticity).

The nonlinearity displayed in the stress–strain curve (Figure 1a), a reversible yield transition, has a degree of universality within the mechanics of large, compact biomolecules, and can be seen dynamically, as in Figure 1a, or also in equilibrium experiments. An example is kinking in short, double-stranded (ds) DNA molecules. Consider a 30-base-pairs (bp) long DNA molecule. It is a nanoparticle roughly in the shape of a cylindrical rod, 10-nm long and 2-nm in diameter. Under a compressive force it buckles, with a free energy roughly described by the elastic bending energy, E_{el} , of a thin rod in the linear elasticity regime:

$$E_{el} = \int_0^L ds \frac{1}{2} B \kappa^2(s), \quad (1)$$

where s is the arclength along the (1D) rod, κ the curvature, B the bending modulus ($B \approx 200$ pN nm² for DNA), and L the length of the rod. However, for a critical value τ_c of the internal bending torque, τ , there is a reversible yield transition, believed to correspond, structurally, to the formation of a kink in the DNA nanorod.⁷ Figure 2a represents an experimental situation where the compressive force on the DNA nanorod is provided by the extension of a single-stranded (ss) DNA “entropic spring.” This configuration (called “D-DNA” because a 90° clockwise rotation of Figure 2a makes it look like the uppercase letter “D”) is easy to obtain by hybridization (i.e., self-assembly) of two synthetic single strands of DNA with opportunely chosen base sequences. Reducing the number of bases, N_s , in the ss part of the construction has the effect of increasing the compressive force on the ds part. Figure 2b shows the corresponding elastic free-energy curve (energy versus N_s) determined experimentally, using a thermodynamic method described in Reference 20 (we gloss over details: for the expert, the measurements of Figure 2b were obtained for D-DNA with a nick at the center of the ds part). It shows a yield transition at $N_s \approx 25$, signaled by the cusp in the curve. Through a minimal model that treats the molecule of Figure 2a as a system of two coupled nonlinear springs (a “leaf spring” for the ds part of the molecule, a “coil spring” for the ss part) one obtains, from the measurements of the elastic energy Figure 2b, the bending energy of the ds DNA versus end-to-end distance, x . It shows that the regime of linear bending elasticity is cut off by a reversible yield transition¹⁹ not unlike the softening transition of Figure 1a.

Coupled nonlinear springs—the Fermi–Pasta–Ulam–Tsingou problem²¹—remain of fundamental interest in nonlinear physics. Connected to nonlinearity at the molecular scale is the question of atomic-scale dissipation in the driven,

out-of-equilibrium system. Dissipation being a collective phenomenon, it is of fundamental interest to observe the atomic-scale mechanisms that result in dissipative dynamics on a larger scale. At what scale does the second law of thermodynamics come into play, the “arrow of time” form? With respect to an enzyme molecule, we may ask: Is the driven (out-of-equilibrium) conformational motion of the molecule dissipative, and can we measure the characteristics and understand the mechanisms of this dissipation?

There are exciting opportunities for new experiments here; as an example, we mention a recent measurement of dissipation at the Angstrom scale by nanorheology. As in a macroscopic rheology experiment, with nanorheology, one has access to the real and the imaginary part of the driven system’s response,

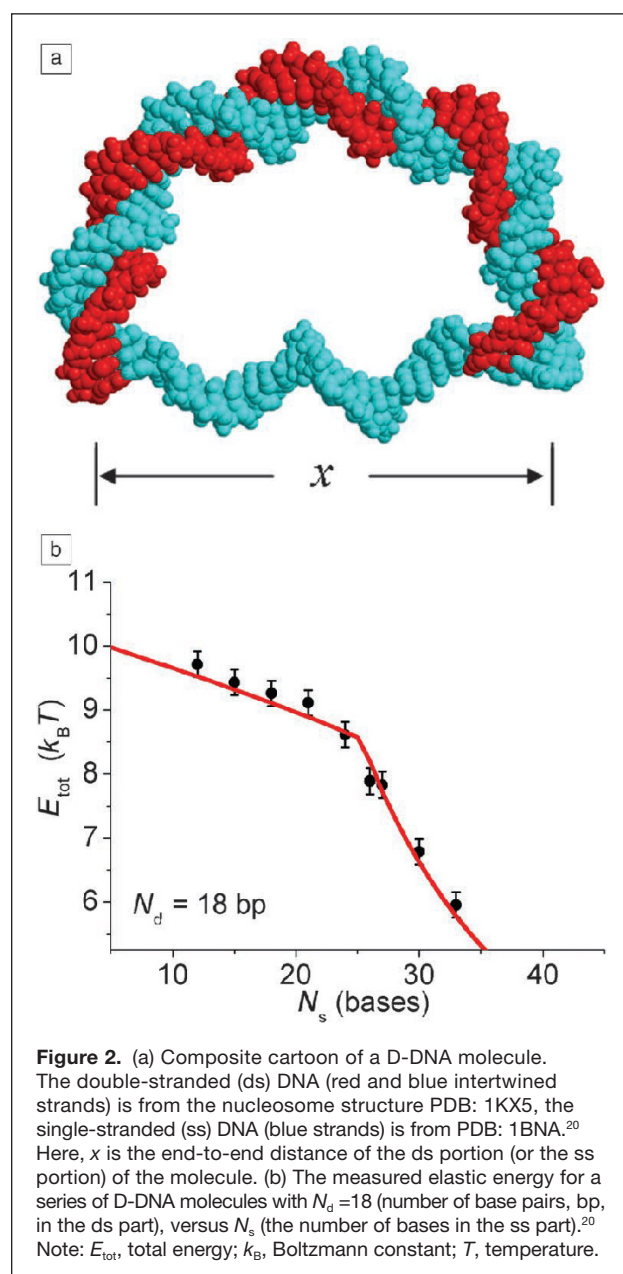


Figure 2. (a) Composite cartoon of a D-DNA molecule. The double-stranded (ds) DNA (red and blue intertwined strands) is from the nucleosome structure PDB: 1KX5, the single-stranded (ss) DNA (blue strands) is from PDB: 1BNA.²⁰ Here, x is the end-to-end distance of the ds portion (or the ss portion) of the molecule. (b) The measured elastic energy for a series of D-DNA molecules with $N_d = 18$ (number of base pairs, bp, in the ds part), versus N_s (the number of bases in the ss part).²⁰ Note: E_{tot} , total energy; k_B , Boltzmann constant; T , temperature.

or equivalently the amplitude and the phase. **Figure 3**²² shows the latter two quantities measured as a function of driving frequency, for the same enzyme of Figure 1. The phase ϕ is the phase difference between the applied sinusoidal force and the measured deformation; $\phi = 0$ corresponds to nondissipative dynamics (the force and the velocity are out of phase), $\phi = -\pi/2$ to maximum dissipation (force and velocity are in phase). For a fixed amplitude of the force, the measured dynamics are described by the Maxwell model of viscoelasticity (solid lines in Figure 3):

$$A = \frac{F_0}{\omega\gamma} \sqrt{1 + \left(\frac{\omega}{\omega_c}\right)^2}, \quad \phi = -\arctan\left(\frac{\omega_c}{\omega}\right), \quad (2)$$

where A is the deformation amplitude, ϕ the phase, F_0 the amplitude of the force, ω the forcing frequency, $\omega_c = \kappa/\gamma$ the corner frequency constructed with the elastic parameter κ , and the dissipative parameter, γ .

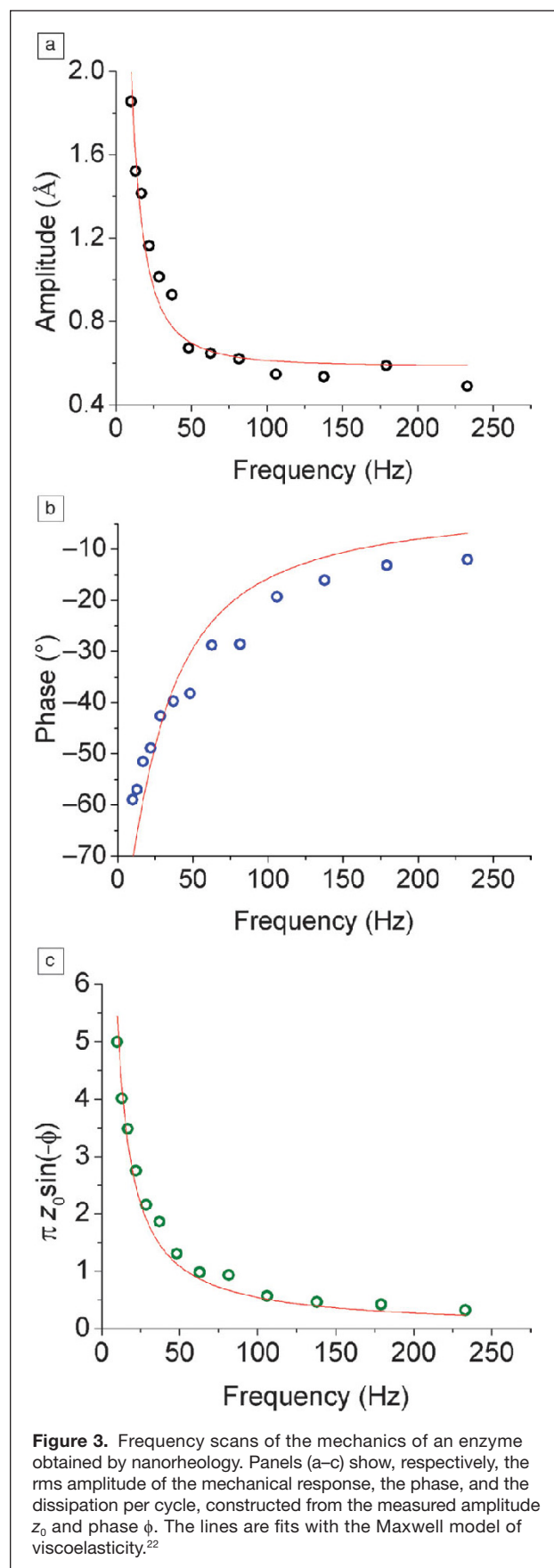
If we assume the Maxwell model, then from the thermodynamic parameters F_0 , A , ϕ (amplitude of the force, the deformation, and phase) we can obtain the dissipation (energy dissipated per cycle) as:

$$\frac{dW}{dt} = \pi F_0 A \sin(-\phi). \quad (3)$$

This quantity is plotted in Figure 3c using the measured values of A and ϕ from Figure 3a–b; the solid line is the Maxwell model prediction. Because the force is not calibrated in the experiments, F_0 is an unknown proportionality constant. In substance, the measurements show that, in this case, dissipation in the driven conformational motion of the molecule follows viscoelastic dynamics (i.e., the dissipation increases at low frequency [the opposite of a damped spring]). These experiments only begin to address the general questions previously discussed. The mechanisms responsible for the measured dissipation are not yet clear. The hydration layer of the enzyme certainly plays an important role: once again, surface dynamics is important for these soft nanoparticles. In conclusion, we see opportunities for innovative studies of atomic-scale friction using these systems.

Composite functional materials: The artificial axon

Any tissue in a living organism is a functional material, organized around a basic unit, which is the cell. This scheme is too complicated to reproduce synthetically, and in any case, why copy nature exactly? On the other hand, opening up the biological cell, extracting only selected molecular components, and reassembling them in a polymer or solid-state matrix seems a viable way forward. The biological components would give the functionality, the polymer, or solid matrix the scaffold. For example, we saw that the catalytic activity of any enzyme can be turned on and off by sufficient mechanical stress on the molecule. This approach then gives



access to order of 10^4 different chemical reactions (all water-based), which can be controlled mechanically. A polymer hydrogel cross-linked by enzymes could in principle be designed such that a given chemical reaction, or even a cascade of reactions, is turned on within the material depending on the state of mechanical stress. Another example is the molecular-scale positioning of an enzyme—and therefore, the locus of a given chemical reaction—through the self-assembly method of the DNA origami (supra-molecular constructions with user-defined three-dimensional (3D) shape and user-defined recognition sites, so that any other (DNA tagged) molecule can be exactly positioned on the structure).^{23–25} One gets the sense that such materials could form the basis for all manner of interesting devices, though which specific applications will emerge is, once again, difficult to predict.

We now look in more detail at a different example. The artificial axon is a synthetic structure that supports action potentials.^{26,27} In its present form, it is a $\sim 100\text{-}\mu\text{m}$ lipid bilayer patch on a solid support, separating a “*cis*” from a “*trans*” oriented aqueous chamber. About 100 voltage-gated potassium channels are inserted in the membrane patch. These transmembrane proteins are pores that, in the open state, are selectively permeable to K^+ ions, with a conductance of order 10 pA/100 mV. Opening and closing of the pore (which can be thought of as a binary stochastic variable) is controlled by the voltage across the bilayer (the voltage difference between the *cis* and *trans* compartments): within an interval of ~ 100 mV, the probability that the channel is open changes smoothly from 0 to 1. A concentration ratio of a factor ~ 10 in KCl is maintained externally between the *cis* and *trans* chambers (e.g., $[K^+]_{trans} = 100$ mM, $[K^+]_{cis} = 10$ mM), giving rise to an equilibrium (Nernst) potential difference V_N across the bilayer according to:

$$V_N = \frac{kT}{|e|} \ln \frac{[K^+]_{trans}}{[K^+]_{cis}} \approx 25\text{mV} \times \ln \frac{[K^+]_{trans}}{[K^+]_{cis}}. \quad (4)$$

Here, k is the Boltzmann constant, T the temperature, and e the charge of the electron. For accuracy, let us ground the *trans* chamber and measure the voltage $V(t)$ of the *cis* chamber. Then in equilibrium, $V(t) = V_N \approx +60$ mV. For $V < -50$ mV, the channels are closed with probability 1; for $V > +20$ mV, they are open with probability 1. If V is held off equilibrium, at a “resting potential,” $V_r = -100$ mV say, the system is unstable against opening of the channels. In the nerve cell, the off equilibrium resting potential is the outcome of a second ionic gradient (of Na^+) opposed to the K^+ gradient. With the channel closed, small leak currents of these ions across the bilayer establish the resting potential. In the artificial axon, the same is achieved by injecting a small “leak current” using a special kind of voltage clamp. The result is a system that displays the same basic electrophysiology characteristics as a real nerve cell—it fires an action potential (a voltage spike of fixed shape) in response to an above-threshold stimulus (Figure 4a), and it fires a train of spikes in response to a constant input current (Figure 4b), the firing rate increasing with

the current. This behavior is referred to as “integrate and fire” in electrophysiology. These are the essential features: a threshold device, allowing for logic operations (such as AND, OR); and integrate and fire, allowing for one axon to process the input of many other axons. A network of such devices has both digital and analog processing power, and so is fundamentally different from both a digital computer and an analog controller.

To connect two artificial axons, one needs a “synapse,” which functionally is a current clamp controlled by the voltage in the presynaptic axon and injecting a corresponding current in the postsynaptic axon. It can be realized by electronics, of course, but the challenge is to realize it through an ionic device matched to the 100 meV energy scale and the 100- μm length scale characteristic of the artificial axon. A further challenge would be to endow this synapse with “plasticity”—the property of changing its strength (the relation between input voltage and output current) depending on the history of usage. At the moment, what stands in the way of realizing a system of more than a few artificial axons is the extremely cumbersome, non-scalable procedure used to obtain a functional supported bilayer with channels, and its fragility. This is a materials science problem in itself, with interesting possible ways forward. For example, one might think of building the solid matrix for a network of artificial axons by adapting the 3D printing technology being developed to steer the growth of neuronal cultures.^{28–30} Robustness might be improved by embedding the bilayer in a polymer matrix.

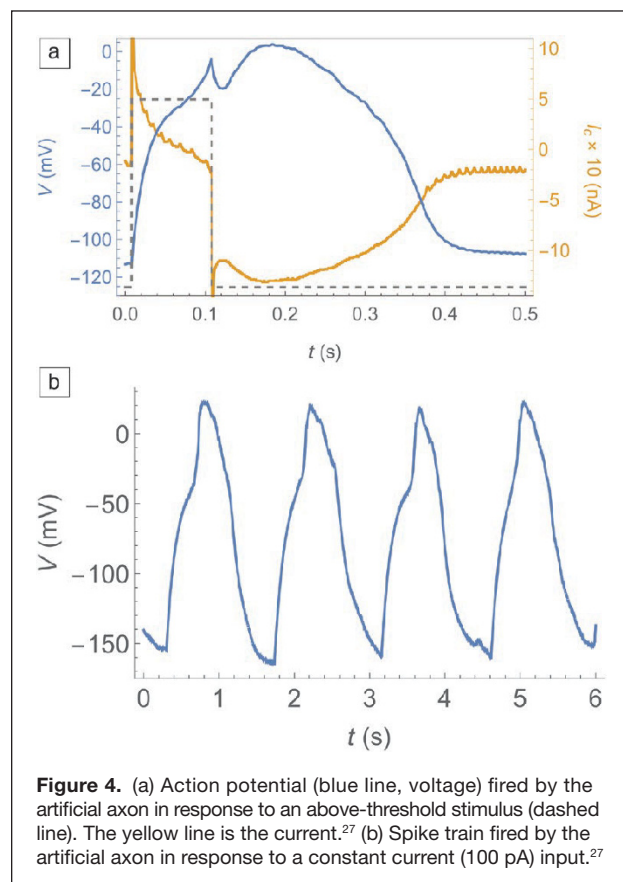


Figure 4. (a) Action potential (blue line, voltage) fired by the artificial axon in response to an above-threshold stimulus (dashed line). The yellow line is the current.²⁷ (b) Spike train fired by the artificial axon in response to a constant current (100 pA) input.²⁷

Let us now imagine that we have the capability of building robust, reasonably large networks of such artificial axons. Devices could presumably be developed, from artificial noses to image recognition units. Sensory inputs are chemically gated, light gated, and pressure gated ion channels, which is how our own senses work. Also, before dismissing this approach as inferior to existing electronic devices, consider that a device running entirely on ionics is, by comparison, low power. The power source is distributed, and runs on, literally, a sea salt gradient. The components are biodegradable, and their method of synthesis biological.

One can debate about future applications, but what seems clear is the opportunity of moving certain basic science areas forward through the constructivist approach embodied in the artificial axon. The basic feature, in this respect, is that the processing power of the artificial axon, like that of our neurons, is neither entirely digital nor entirely analog—it is mixed. We feel there are opportunities here for a new angle of inquiry combining the fields of nonlinear dynamics, dynamical systems, control theory, and algorithmic mathematics. For example, suppose we want to make an autonomous control mechanism to steer a toy car toward a light source. The car has a right eye and a left eye, and we use a control system built with two artificial axons. The connections are such that when the right eye sees light, it inputs current into the right axon, which starts to fire at a corresponding rate. Same for the left eye and axon. Further, if the right axon fires a spike, the wheels of the car turn right, and if the left axon fires, they turn left. This kind of vehicle is the first in a series of increasing complexity presented (from a cybernetics/neurobiology perspective) in the book by V. Breitenberg titled *Vehicles*.³¹ We focus on the axons: part of their processing is analog, namely the firing rate that increases with increasing input current. And part is digital: The axon fires or does not fire (a yes or no event) and correspondingly, the wheels turn or stay put (a yes or no event). From the point of view of nonlinear dynamics, this mixed behavior comes about because the firing of an action potential corresponds to a saddle node bifurcation, exhibiting critical slowing down near the critical point. Now it turns out that this system, which has actually been implemented in this author's lab,³² does in fact steer the car. The mechanism is not so obvious. It relies mainly on the relative phase of the spikes in the right and left axons. Thus, while the algorithm is simple, an analytical understanding of how it works is not.

Extrapolating to a more complex, “brain-like” network, we feel that there is no hope for an analytical understanding of “how it works,” whereas an understanding of the algorithms is possible. Coming back to the two axons and the car, this is already a quite interesting dynamical system. One can ask, for example, about the robustness of the steering mechanism. In dynamical systems language, what is the basin of attraction in parameter space (speed of the car and firing rates of the axons) of the limit cycle, which is the desired end state (the car moving in a circle that contains the light source)? Such questions are easy to assess by simulating the system, but hard to assess analytically. In conclusion, these systems offer an opportunity for experimentalists to advance a

kind of modern cybernetics or algorithmic mathematics based on mixed analog and digital processes.

Acknowledgments

We gratefully acknowledge support from the National Science Foundation under Grant No. DMR-1809381.

References

1. E. Drexler, C. Peterson, G. Pergamit, *Unbounding the Future: The Nanotechnology Revolution* (William Morrow, New York, 1991).
2. F. Huber, J. Schnaubl, S. Röncke, P. Rauch, K. Müller, C. Fütterer, J. Käs, *Adv. Phys.* **62**, 1 (2013).
3. B.H. McMahon, F.G. Parak, P.W. Fenimore, H. Frauenfelder, *Proc. Natl. Acad. Sci. U.S.A.* **99**, 16047 (2002).
4. H. Frauenfelder, G. Chen, J. Berendzen, P.W. Fenimore, H. Jansson, B.H. McMahon, I.R. Stroe, J. Swenson, R.D. Young, *Proc. Natl. Acad. Sci. U.S.A.* **106**, 5129 (2009).
5. L. Wanga, Y. Qina, D. Zhong, *Proc. Natl. Acad. Sci. U.S.A.* **113**, 8424 (2016).
6. J. Yang, Y. Wang, L. Wang, D. Zhong, *J. Am. Coll. Surg.* **139**, 4399 (2017).
7. G. Zocchi, *Molecular Machines, a Materials Science Approach* (Princeton University Press, Princeton, NJ, 2018).
8. D.E. Koshland Jr., *Proc. Natl. Acad. Sci. U.S.A.* **44**, 98 (1958).
9. T.A. Steitz, W.F. Anderson, R.J. Fletterick, C.M. Anderson, *J. Biol. Chem.* **252**, 4494 (1977).
10. W.S. Bennett, T.A. Steitz, *Proc. Natl. Acad. Sci. U.S.A.* **75**, 4848 (1978).
11. B. Choi, G. Zocchi, S. Canale, Y. Wu, S. Chan, L.J. Perry, *Phys. Rev. Lett.* **94**, 038103 (2005).
12. Y. Wang, G. Zocchi, *Phys. Rev. Lett.* **105**, 238104 (2010).
13. D.R. Hekstra, K.I. White, M.A. Socolich, R.W. Henning, V. Šrajer, R. Ranganathan, *Nature* **540**, 400 (2016).
14. C.-Y. Tseng, A. Wang, G. Zocchi, *Europhys. Lett.* **91**, 18005 (2010).
15. C.-Y. Tseng, G. Zocchi, *J. Am. Coll. Surg.* **135**, 11879 (2013).
16. Y. Wang, G. Zocchi, *Europhys. Lett.* **96**, 18003 (2011).
17. Y. Wang, G. Zocchi, *PLoS One* **6** (12), e28097 (2011).
18. A. Ariyaratne, C. Wu, C.-Y. Tseng, G. Zocchi, *Phys. Rev. Lett.* **113**, 198101 (2014).
19. H. Qu, J. Landy, G. Zocchi, *Phys. Rev. E Stat. Nonlin. Soft Matter Phys.* **86**, 041915 (2012).
20. H. Qu, G. Zocchi, *Europhys. Lett.* **94**, 18003 (2011).
21. T. Dauxois, *Phys. Today* **61**, 55 (2008).
22. Z. Alavi, G. Zocchi, *Phys. Rev. E Stat. Nonlin. Soft Matter Phys.* **97**, 052402 (2018).
23. P.W.K. Rothmund, *Nature* **440**, 297 (2006).
24. W.M. Shih, J.D. Quispe, G.F. Joyce, *Nature* **427**, 618 (2004).
25. J. Chen, N.C. Seeman, *Nature* **350**, 631 (1991).
26. A. Ariyaratne, G. Zocchi, *J. Phys. Chem. B* **120**, 6255 (2016).
27. H.G. Vasquez, G. Zocchi, *Europhys. Lett.* **119**, 48003 (2017).
28. C.M. O'Brien, B. Holmes, S. Faucett, L.G. Zhang, *Tissue. Eng. Part B Rev.* **21** (1), 103 (2015).
29. M. Thomas, S.M. Willerth, *Front. Bioeng. Biotechnol.* **5**, 69 (2017).
30. D. Espinosa-Hoyos, A. Jagielska, K.A. Homan, H. Du, T. Busbee, D.G. Anderson, N.X. Fang, J.A. Lewis, K.J. Van Vliet, *Sci. Rep.* **8**, 478 (2018).
31. V. Braitenberg, *Vehicles* (MIT Press, Cambridge, MA, 1984).
32. H.G. Vasquez, G. Zocchi, *Bioinspir. Biomim.* **14**, 016017 (2019). □



Giovanni Zocchi has been a professor in the Department of Physics at the University of California, Los Angeles, since 1999. He received his BS degree in physics at the Università di Pisa and Scuola Normale Superiore, Italy. He obtained his PhD degree in physics from The University of Chicago in 1990. He completed postdoctoral research at the École Normale Supérieure, France, from 1990 to 1993. He joined the Niels Bohr Institute in Copenhagen, Denmark, as an assistant professor from 1994 to 1999. His research focuses on mechanochemical coupling in enzymes, and he pioneered the artificial mechanical control of enzymes. He was awarded

the 2017 Feynman Prize in Nanotechnology (theory). Zocchi can be reached by email at zocchi@physics.ucla.edu.